X-RAY DIFFRACTION STUDY OF LIQUID-PHASE SINTERED PERMANENT MAGNETS OF RCo_5 TYPE

YUAN CHUN-HUA (袁重华), PAN CHUN-YEN (潘崇言),
CHIN JUEI-HSIANG (金瑞湘), AND WU LIN-WEI (吴灵葳)
(Research Institute of Iron and Steel, Ministry of Metallurgy)

Received Jan. 11, 1974.

ABSTRACT

X-ray diffraction study, together with magnetic measurements, was made on liquid-phase sintered permanent magnets of the RCo_5 type (R = Sm, $Sm_{0.5}$ $Pr_{0.5}$, or $MM_{0.6}$ $Sm_{0.5}$). It was found that the sintered samples invariably possessed a skin layer of about 0.3 mm in thickness. This layer and the core of the sample, therefore, had to be studied separately, magnetic measurements being made only on the core. In comparison with the core, the skin layer proved to have a more complex structure. As far as composition is concerned, the skin material had a higher R-content and a lower Co-content. At an overall Co-content of about 63% by weight, the sintered core had a maximum intrinsic coercive force and exhibited only a single metallic phase, i.e., the RCo_5-type intermetallic compound with $CaZn_5$ structure. No evidence for the presence of any R_2Co_7 or R_2Co_{17} phase was detected in the diffraction patterns. The relative amount of the liquid-phase sintering aid in the mixed powder before sintering was varied in order to obtain a series of compacts of different overall Co-contents. Sintered cores from powder compacts of overall Co-contents different from the optimum (63 wt.%) generally showed the presence of a second metallic phase. As soon as a second phase appeared, whether it was R_2Co_7 or R_2Co_{17}, the magnetic properties of the sintered core became inferior to those of a sample of the optimum composition. Moreover, the magnetic parameters of the sintered core varied monotonically with the relative content of the second phase. On the basis of these findings, a model of the mechanism of liquid-phase sintering is tentatively suggested. It is pointed out that absence of the R_2Co_7 phase in the sintered core possessing the maximum coercive force is in obvious disagreement with the epitaxial shell model recently proposed by Strnat and co-workers.

INTRODUCTION

It is now well known that consolidated powders of rare-earth-cobalt alloys of RCo_5 type (R = La, Ce, Pr, Nd, Sm, etc.) belong to a group of permanent magnets far superior in certain important respects to the best conventional permanent magnet materials. In recent years, these permanent magnets have been widely prepared by a liquid-phase sintering technique. The mechanism of this kind of sintering process and the changes in the phase constitution of the alloy during the process, the correlation between the phase constitution and the magnetic properties of the sintered sample, and the mechanism that gives rise to high coercive force are problems of recent interest, to which a great deal of work has been devoted.

Benz and Martin[1], studying the volume shrinkage and the development of high coercive force during sintering, have postulated a model for the mechanism of

shrinkage, on the basis of which it is conceived that the high coercive force structures achieved in these alloys would be those with a relatively high concentration of cobalt-vacancies in the grain boundary regions. Their optical and electron microscopic observations showed, however, that the grain boundary regions of the sintered alloys were largely free from defects. The defective structures which cause wall-pinning at the grain boundary regions are, therefore, presumed to be of atomic level. They have not considered the direct effect of the presence of a second magnetic phase on the average magnetic properties of the sintered alloy.

Strnat and co-workers[2,3] have studied the variation of the coercive force with the sintering or annealing temperature and, in interpreting the results obtained, have suggested that during liquid-phase sintering a highly defective epitaxial layer of the R_2Co_7 phase forms on the surface of the quite perfect single-domain grains of the matrix RCo_5 phase. The wall-pinning sites reside in the epitaxial shell. According to this model, the development of a high coercive force should depend upon the presence of a considerable amount of the second magnetic phase R_2Co_7.

The present work aims mainly to obtain correlations between the phase constitution and the magnetic properties of liquid-phase sintered alloys of various compositions by making X-ray diffraction studies and magnetic measurements on the same samples. It is hoped that the results of such a study will be beneficial to the improvement of the preparation technology and of the magnetic properties of this type of permanent magnets.

Experimental

Three kinds of permanent magnet alloys have been studied, namely, $SmCo_5$, $Sm_{0.5}Pr_{0.5}Co_5$, and $MM_{0.5}Sm_{0.5}Co_5$ (MM denotes cerium-rich misch metal). The compositions of the base alloys are nearly stoichiometric in accordance with these formulas and that of the liquid-phase sintering aid is 60% Sm and 40% Co by weight for all three kinds. Both base alloys and sintering additive were prepared in an intermediate frequency vacuum induction furnace. The ingots were crushed and milled into powders of $1\sim10\mu m$ particle size. Each of the base alloy powders was then blended in different proportions with powders of the sintering aid, so that a series of powder mixtures of overall Co-contents of 57, 59, 62, 63, 65, and 67% by weight was obtained. Cylinders of Ø8.5 mm × 6 mm were compressed from these mixed powders in a magnetic field, sintered under an argon atmosphere at about 1100°C for 30—60 min, and subsequently cooled in vacuum or alcohol. The sintered samples thus obtained invariably had a skin layer of about 0.3 mm in thickness. A line of division between the skin and the core on the end of a cylinder could be distinctly discerned by naked eye. The skin material was carefully taken off the core, which was used first for magnetic measurement. Subsequently, both the skin material and the core were pulverized into particles of micron order for X-ray diffraction study. Powder patterns were taken by an Enraf-Nonius Guinier Type-II camera, using Co-K_α radiation and an exposure of 4—9 hr.

In order to evaluate the relative variations in the contents of alloy phases in the samples, the (202) line of the R_2Co_7 phase and the (111) line of the RCo_5 phase were recorded simultaneously by a diffractometer, using a 2½°–2°–0.2° slit system, a

scanning rate of 0.5 degree/minute, $Cr - K_\alpha$ radiation, and vanadium filter. The relative content of a phase is thus represented by the ratio of integrated intensity of an appropriate line.

However, the (202) line of R_2Co_7 and the (111) line of RCo_5 are partly overlapped, so that successive approximation by a method of asymptotic plotting was employed to separate them. This was carried out as follows: Let $\varphi(\theta)$ and $f(\theta - \chi)$ denote the intensity functions of the true lines respectively. Draw lines from the vertices of the two peaks in the diffraction pattern perpendicular to the θ-axis. Regrading these lines as the axes of symmetry of the respective lines, zero order approximations can be obtained from the "unoverlapped" halves in the pattern (the lines are, of course, assumed to be symmetical). Denoting these by $\varphi_0(\theta)$ and $f_0(\theta - \chi_0)$ respectively, we obviously have

$$\varphi_0(\theta) > \varphi(\theta) \text{ and } f_0(\theta - \chi_0) > f(\theta - \chi).$$

Using the zero order approximations as a beginning, higher order approximations can be successively plotted out, such that

$$f_{i+1}(\theta + \chi_{i+1}) = f_0(\theta - \chi_0) - \varphi_i(\theta),$$
$$\varphi_{i+1}(\theta) = \varphi_0(\theta) - f_i(\theta - \chi_i).$$

Thus two series of intensity functions are obtained, satisfying

$$f_0 > f_2 > f_4 \cdots > f_{2n} > f > f_{2n+1} > \cdots f_5 > f_3 > f_1,$$
$$\varphi_0 > \varphi_2 > \varphi_4 \cdots > \varphi_{2n} > \varphi > \varphi_{2n+1} > \cdots \varphi_5 > \varphi_3 > \varphi_1.$$

The plotting continues until the axes of symmetry of the plotted lines no longer move and the curve plotted from the sum $\varphi(\theta) + f(\theta - \chi)$ become equal to the recorded pattern.

The sintered cores used for magnetic measurements were of 8.5 mm diameter and 6 mm length. They were first magnetized in a pulsed field of over 10^5 oersteds and their second-quadrant demagnetization curves were traced out by a dc hysteresigraph.

Compositions of alloys and sintered materials were analyzed by X-ray fluorescence.

Results

As optimum magnetic properties were obtained in the cores of sintered samples of 63 wt.% overall Co-content for all three kinds of alloys, we shall first describe the results obtained from samples of this overall Co-content as a group. Eight Guinier patterns are grouped together in Plate I for comparison. The first four patterns are from the $MM_{0.5}Sm_{0.5}Co_5$ base alloy, an $MM_{0.5}Sm_{0.5}Co_5$ liquid-phase sintered core, the powder mixture of $MM_{0.5}Sm_{0.5}Co_5$ base alloy plus Sm–Co sintering aid before sintering, and the Sm–Co sintering aid, respectively. Patterns from liquid-phase sintered cores of the $Sm_{0.5}Pr_{0.5}Co_5$ and the $SmCo_5$ kinds are given as *e* and *f* respectively. Patterns from the skin materials of liquid-phase sintered samples of all three kinds of alloys are nearly identical and, therefore, only a pattern from the skin material of a sintered $MM_{0.5}Sm_{0.5}Co_5$ sample is shown, which is designated Pat-

tern *g*. A portion of a powder mixture of $MM_{0.5}Sm_{0.5}Co_5$ plus Sm–Co sintering aid was burnt completely in air at 1095°C and a pattern was obtained from the residue; this is Pattern *h* of Plate I. The purpose of obtaining this last pattern will be seen in the following.

Plate II is a comparison of Guinier patterns from liquid-phase sintered $Sm_{0.5}Pr_{0.5}Co_5$ cores of different overall Co-contents. Note that the base alloy alone has an overall Co-content of 67 wt.%.

Plate III shows the variation of the recorded diffraction lines from liquid-phase sintered $Sm_{0.5}Pr_{0.5}Co_5$ cores with the composition of the sample. Plate IV shows the recorded diffraction lines from a part of the samples seen in Plate III after annealing at 900°C.

Data derived from patterns of Plate I for the RCo_5 phases in sintered cores of optimum composition are listed in Tables 1 to 3. Also, data for three phases identified in Pattern *a* of Plate II are llisted in Table 4; and those for two phases identified in Pattern *e* of Plate II in Table 5.

Table 1

Powder Pattern Data of Liquid-Phase Sintered $MM_{0.5}Sm_{0.5}Co_5$ Core

Overall Co-content of powder compact: 63 % by weight
Sintering temperature: 1095°C
Guinier II camera, 5 hrs. CoK_α
$CaZn_5$ type structure: $a = 4.95$ Å, $c = 3.94$ Å, $c/a = 0.80$

(*hkl*)	$\sin^2\theta_{Calcd}$	$\sin^2\theta_{Meas}$	I_{Meas}
100	0.0437	0.0432	W
001	0.0575	0.0514	W
101	0.0952	0.0955	W
110	0.1311	0.1308	M
200	0.1748	0.1746	S
111	0.1826	0.1826	VS
002	0.2058	0.2061	M
201	0.2262	0.2262	W
112	0.3369	0.3372	M
211	0.3574	0.3588	M
202	0.3806	0.3824	M
300	0.3933	0.3968	W
301	0.4448	0.4477	M

Results of magnetic measurements are presented only for the sintered $Sm_{0.5}Pr_{0.5}Co_5$ magnets, since the results for the other two series of alloys are quite similar. The magnetic parameters are plotted as functions of the overall Co-content in Fig. 1. They are plotted as functions of the relative content of the R_2Co_7 phase in Fig. 2

Table 2

Powder Pattern Data of Liquid-Phase Sintered $Sm_{0.5}Pr_{0.5}Co_5$ Core

Overall Co-content of powder compact: 63 % by weight

Sintering temperature: 1130 °C

Guinier II camera, 5 hr. CoK_α

$CaZn_5$ type structure:

$a = 4.99$ Å, $c = 3.96$ Å, $c/a = 0.79$

(hkl)	$\sin^2\theta_{Calcd}$	$\sin^2\theta_{Meas}$	I_{Meas}
100	0.0431	0.0432	W
001	0.0512	0.0510	W
101	0.0943	0.0945	S
110	0.1293	0.1290	M
200	0.1724	0.1720	S
111	0.1805	0.1813	VS
002	0.2048	0.2061	M
201	0.2236	0.2233	W
112	0.3341	0.3339	M
211	0.3529	0.3538	M
202	0.3772	0.3790	M
300	0.3879	0.3892	W
301	0.4391	0.4425	M

Table 3

Powder Pattern Data of Liquid-Phase Sintered $SmCo_5$ Core

Overall Co-content of powder compact: 64 % by weight

Sintering temperature: 1160 °C

Guinier camera, 5 hr. CoK_α

$CaZn_5$ type structure:

$a = 4.99$ Å, $c = 3.99$ Å, $c/a = 0.80$

(hkl)	$\sin^2\theta_{Calcd}$	$\sin^2\theta_{Meas}$	I_{Meas}
100	0.0429	0.0425	W
001	0.0502	0.0498	W
101	0.0931	0.0930	S
110	0.1287	0.1284	M
200	0.1716	0.1719	S
111	0.1789	0.1786	VS
002	0.2008	0.2018	M
201	0.2218	0.2218	W
112	0.3295	0.3306	M
211	0.3505	0.3521	M
202	0.3724	0.3739	M
300	0.3861	0.3892	W
301	0.4363	0.4408	M

Table 4

Powder Pattern Data of Liquid-Phase Sintered $Sm_{0.5}Pr_{0.5}Co_5$ Core

Overall Co-content of powder compact: 59 % by weight

Sintering temperature, 1130 °C; sintering time, 1 hr; cooled in alcohol

RCo_5 phase: $CaZn_5$ type structure $a = 4.98$ Å, $c = 3.69$ Å, $c/a = 0.79$

R_2Co_7 phase: $a = 5.00$ Å, $c = 22.96$ Å, $c/a = 4.60$

RCo_5 modification: $a = 9.85$ Å, $c = 7.94$ Å, $c/a = 0.806$

RCo_5		$\sin^2\theta_{Meas}$	I_{Meas}	R_2Co_7	
hkl	$\sin^2\theta_{Calcd}$			$\sin^2\theta_{Calcd}$	*hkl*
100	0.043	0.045	VW		
001	0.051	0.051	VW		
101	0.094	0.094	S		
300	0.101	0.101*	W		
301	0.111	0.109*	W		
003	0.114	0.115*	W		
		0.127	S	0.128	110
110	0.129	0.129	M		
		0.170	S	0.170	200
200	0.172	0.172	M		
		0.176	VS	0.176	202
111	0.180	0.180	VS		
		0.196	W	0.195	204
002	0.204	0.204	VW		
201	0.223	0.223	W		
112	0.333	0.335	W		
211	0.352	0.354	W		
202	0.376	0.378	W		
300	0.387	0.390	W		
		0.435	W	0.439	306
301	0.438	0.442	M		

* After Ref. [4].

and of that of the RCo_5 phase in Fig. 3. The values of these relative contents are derived from the ratio of integrated intensities of the diffraction lines, as has been mentioned above. Note that these are normalized values, taking the content of the R_2Co_7 phase in the 57 wt.% Co sample and that of the RCo_5 phase in the 63 wt.% Co sample as unity.

The relative contents of both the R_2Co_7 and RCo_5 phases in the as sintered cores changed after annealing at 900°C. This is illustrated in Fig. 4.

The salient points brought out by the experimental results described above can be summarized as follows.

(1) When optimum magnetic properties are obtained in a liquid-phase sintered core of the RCo_5 type, it contains only a single metallic phase, i.e., the RCo_5 intermetallic compound of hexagonal $CaZn_5$ type structure (see Patterns *b*, *e*, *f* of Plate I;

Table 5

Powder Pattern Data of Liquid-Phase Sintered $Sm_{0.5}Pr_{0.5}Co_5$ Core*
Overall Co-content of powder compact: 67 % by weight
Sintering temperature, 1130 °C; sintering time, 1 hr; cooled in alcohol
RCo_5 phase: $CaZn_5$ type structure $a = 4.99$Å , $c = 3.97$ Å, $c/a = 0.79$
R_2Co_{17} phase: Th_2Zn_{17} type structure $a = 8.4019_6$ Å, $c = 12.2307$ Å, $c/a = 1.4557$

RCo_5		$\sin^2\theta_{Calcd}$	I_{Meas}	R_2Co_{17}*	
(*hkl*)	$\sin^2\theta_{Calcd}$			$\sin^2\theta_{Calcd}$	(*hkl*)
100	0.0426	0.0432	VW		
001	0.0509	0.0506	VW		
101	0.0935	0.0935	VS		
		0.0954	W	0.0936	113
		0.1017	VW	0.1009	104
		0.1114	VW	0.1114	211
110	0.1278	0.1296	M		
		0.1367	M	0.1363	030
		0.1464	M	0.1462	024
200	0.1704	0.1706	M		
111	0.1787	0.1786	VS		
		0.1813	M	0.1816	220
		0.1840	M	0.1843	033
		0.1949	W	0.1944	205
002	0.2036	0.2033	M		
201	0.2213	0.2248	W		
		0.2306	M	0.2298	223
		0.2439	VW	0.2475	401
112	0.3314	0.3306	M		
211	0.3491	0.3530	M		
		0.3672	VW	0.3660	143
		0.3706	VW	0.3684	217
202	0.3740	0.3774	M	0.3744	226*
300	0.3834	0.3883	VW		
301	0.4343	0.4425	M		

* After Ref. [5].

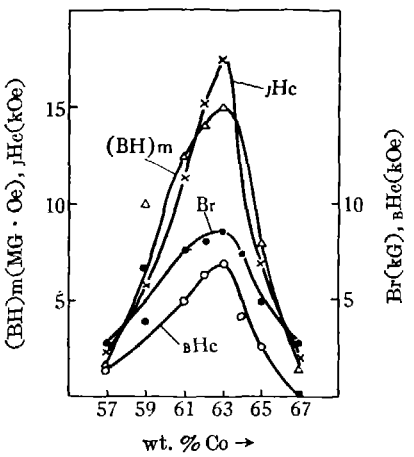

Fig. 1. Intrinsic coercive force $_jH_c$, coercive force $_bH_c$, remanence Br, and maxinum energy product (BH)m of liquid-phase sintered $Sm_{0.5}Pr_{0.5}Co_5$ cores vs cobalt content of the powder compacts.

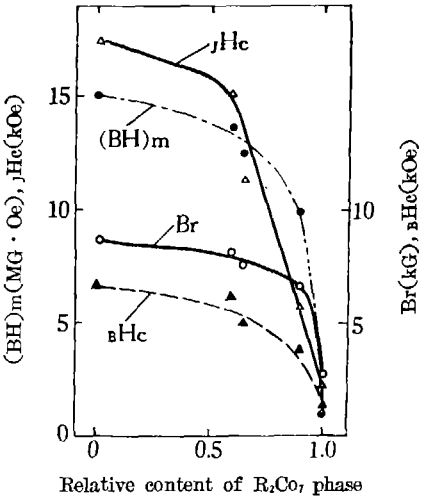

Fig. 2. Magnetic parameters of liquid-phase sintered $Sm_{0.5}Pr_{0.5}Co_5$ cores vs relative content of the R_2Co_7 phase in the cores (taking the R_2Co_7 content in the sintered 57 wt. % Co powder compact as unity).

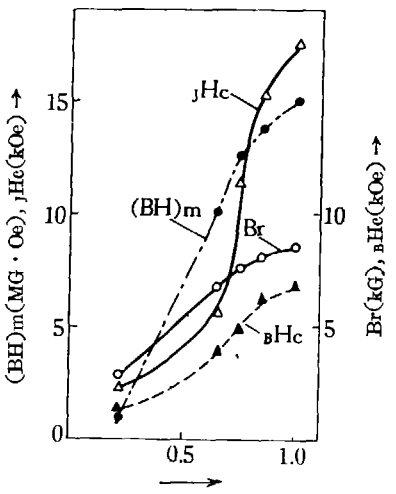

Fig. 3. Magnetic parameters of liquid-phase sintered $Sm_{0.5}Pr_{0.5}Co_5$ cores vs relative content of the RCo_5 phase in the cores (taking the RCo_5 content of the sintered 63 wt. % Co powder compact as unity).

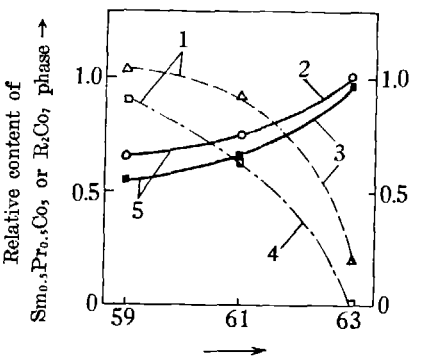

Fig. 4. Change in the relative content of the $Sm_{0.5}Pr_{0.5}Co_5$ or the R_2Co_7 phase in liquid-phase sintered $Sm_{0.5}Pr_{0.5}Co_5$ cores caused by annealing at 900°C (taking the $Sm_{0.5}Pr_{0.5}Co_5$ content of the as sintered 67 wt. % Co core and the R_2Co_7 content of the as sintered 57 wt. % Co core as unity).
(1) R_2Co_7 phase,
(2) (4) As sintered,
(3) Annealed after sintering,
(5) $Sm_{0.5}Pr_{0.5}Co_5$ phase.

Pattern *c* of Plate II; the recorded line from the 63 wt.% Co sample in Plate III; and Fig. 1.). No lines of any other phase are detected in its Guinier pattern. This holds for $SmCo_5$ and $MM_{0.5}Sm_{0.5}Co_5$ as well as for $Sm_{0.5}Pr_{0.5}Co_5$.

(2) Diffraction lines from the liquid-phase sintering aid can be seen clearly in Pattern *c* of Plate I for the mixed powder before sintering, but no traces of these lines remain after the powder has been sintered. No new lines are detected from the as sintered sample either.

(3) Pattern *g* of Plate I shows that the skin material of a sintered sample is considerably more complex than the core material. It was thought that the skin material consisted mostly of oxides, so that a portion of the powder mixture of 63 wt.% overall Co-content was burnt in air at 1095°C for a sufficiently long time and a diffraction pattern was taken of the residue. Comparison of this pattern (*h* of Plate I) with Pattern *g* of Plate I indicates that the latter contains some extra lines besides those of the oxides of the completely oxidized powder. However, the number of these extra lines is too few to enable us to identify their origin. Chemical analysis gives the composition of the skin material as 58 wt.% Co, 21.8 wt.% Sm, the rest being MM. This indicates that compared to the core, the skin has a lower Co-content and a higher total rare-earth content.

(4) When the overall Co-content of the mixed powder is varied from the optimum (63 wt.%) by varying the proportion of the liquid-phase sintering aid added, a second alloy phase generally appears in the sintered core, as is evidenced by Plate II. The appearance of a second alloy phase is accompanied by a deterioration of the magnetic properties of the sintered core (see Fig. 1).

(5) When the overall Co-content of the mixed powder is below optimum, the second alloy phase that appears in the sintered core is the R_2Co_7 phase (see Plate III). As the overall Co-content decreases and the relative content of the R_2Co_7 phase increases, the magnetic parameters of the sintered core decrease monotonically (Plate III and Fig. 2). On the other hand, with increasing Co-content and increasing relative content of the RCo_5 phase, the increase of the magnetic parameters is also monotonic. Similar results are obtained in the cases of the $SmCo_5$ and $MM_{0.5}Sm_{0.5}Co_5$ magnets.

(6) When not enough or none of the liquid-phase sintering aid is added to the mixed powder (e.g., the samples of overall Co-content 65 wt.% and 67 wt.%), an R_2Co_{17} phase appears in the sintered core, and this is also accompanied by a deterioration of the magnetic properties. (Plate II).

(7) When the cores of the sintered $Sm_{0.5}Pr_{0.5}Co_5$ magnets are annealed at 900°C, the magnetic properties of the cores deteriorate rapidly. From a comparison of Plates IV and III, it can be inferred that this is caused by a general increase or appearance of the R_2Co_7 phase.

Discussions

(1) From the first three points summarized in the last section, it is evident that during sintering the liquid-phase sintering aid disappears and a layer rich in rare-earth forms at the surface of the sample. When the final constitution of the sintered core is approximately a single RCo_5 phase of $CaZn_5$-type structure, all three

magnetic parameters reach their maximum values. The following picture of the sintering process probably explains how all this occurs.

During powder preparation, the alloy particles must be oxidized at the surface and become wrapped in a rare-earth oxide shell. Immediately inside the shell, the alloy becomes lower in rare-earth content than in the inner part. Oxygen is also adsorbed on the surface of the particles to a certain extent. At the sintering temperature, the Sm-rich liquid-phase sintering aid becomes molten and a part of its Sm-content goes to react with the oxygen freed from adsorption. In the meantime, the oxide shells on the base alloy particles break and another part of the samarium content of the liquid phase goes to replenish the rare-earth depleted surface of the base alloy particles. This probably takes place by some mechanism such as the reaction diffusion.

While all this proceeds, the samarium content of the liquid phase decreases and the melting point of it raises steadily. When a sufficient degree of supercooling is reached, precipitation by epitaxial growth on the surface of base alloy grains begins. The solid phase that forms from the liquid phase is probably closer to Sm Co_3 than to Sm_2Co_7 or $SmCo_5$ at first, but as sintering goes on, transformation may continue by reaction diffusion. The end products (single-phase RCo_5 or its mixtures with R_2Co_7 or R_2Co_{17}) of the sintering process obviously depend upon the relative oxygen-content in the sample and powder mixtures of overall Co-contents. Unfortunately, oxygen analysis of our samples is not available at present, so that no attempt has been made to calculate the amounts of the various phases in specific cases.

Since the crystallization process has in itself a purifying effect, most of the impurities and oxides would probably move through the network of grain boundaries as sintering goes on, and would pour onto the surface of the sample. In the same time, the tendency toward equilibrium causes the grains in the inner part of the sample to grow to more perfection. This is evidenced by Benz and Martin's observations mentioned earlier.

(2) Inasmuch as the intrinsic coercive force of a grain depends on its size as well as the conditions of its surface, one cannot in general exclude the possibility that the sintering process affects changes in the average coercive force of a sample through changes in average size as well as average surface conditions of the grains of the main magnetic phase. However, in case where a second phase of different magnetic properties is present to considerable proportions, the simple effect of "mixing" is likely to become dominant.

In the case of the alloys studied in the present work, since the sintering temperature is well below the peritectic temperature of the base alloy and the sintering time is not very long, the grains of the base alloy should not be greatly affected structurally. Furthermore, it is known that the coercive forces of the rare-earth-cobalt intermetallic compounds are intimately connected with their anisotropic fields and that the magnetic anisotropy of the RCo_5 phase is greater than either that of the R_2Co_7 phase or that of the R_2Co_{17} phase. For these reasons, it may be concluded that the variation of the magnetic parameters with the composition or the phase-constitution of the sample shown in Figs. 1—3 is a direct consequence of the presence and the variation of the amount of a second magnetic phase. For overall Co-contents less than 63 wt.%, it is clear from Plates II and III that the second magnetic phase is R_2Co_7.

For the samples of 65 wt.% and 67 wt.% overall Co-content, the second magnetic phase is R_2Co_{17}. But, owing to the existence of a narrow homogeneity region around RCo_5 at high temperatures, an R_2Co_{17} phase may not precipitate out in the 65 wt.% Co sample at the sintering temperature; and when its small amount precipitates during cooling, it is probably highly dispersed. For this reason, we observe in Pattern *d* of Plate II only a shift of the diffraction lines. However, for the 67 wt.% Co sample, the diffraction lines of the R_2Co_{17} phase are quite clear in Pattern *e* of Plate II.

(3) According to the more recent versions of the phase diagram of the Sm–Co system, there is a narrow homogeneity region around $SmCo_5$ at high temperatures which tapers off to the $SmCo_5$ line at lower temperatures. At the sintering temperature, the stable composition of the base alloy may extend, say, from $RCo_{5-\chi}$ to $RCo_{5+\chi}$. An as sintered sample may consist mainly of an alloy phase $RCo_{5-\chi}(\chi < \chi_1)$, which has not come to equilibrium. When the sample is annealed at an elevated temperature below the sintering temperature, this phase may break up into an RCo_5 and an R_2Co_7 phase, i.e.,

$$\alpha RCo_{5-x} \rightarrow \beta RCo_5 + \gamma R_2Co_7.$$

This is probably just the situation that occurred to the sintered $Sm_{0.5}Pr_{0.5}Co_5$ sample of 63 wt.% overall Co-content on annealing at 900°C. A comparison of Plate IV with Plate III shows indeed that on annealing the as sintered samples at 900°C, there is in general some more of the R_2Co_7 phase precipitating out from the main phase ($RCo_{5-\chi}$).

(4) According to the epitaxial shell model of liquid-phase sintering of the $SmCo_5$-type magnets proposed by Strnat and co-workers[2,3], the wall-pinning sites are located in the highly defective epitaxial shells of R_2Co_7 on the surface of the RCo_5 grains. This requires a considerable amount of the R_2Co_7 phase to precipitate out before the coercive force of the sample reaches a maximum. This is in disagreement with the experimental findings of the present work.

Summary

(1) The liquid-phase sintered RCo_5-type permanent magnets studied are found to have a thin skin layer which is comparatively rich in rare-earth and low in cobalt. Optimum magnetic properties are obtained in the sintered core when it consists essentially of a single RCo_5 phase of $CaZn_5$-type structure. This requires that a right proportion of liquid-phase sintering aid be present in the powder mixture before sintering, but this proportion also depends on the oxygen content in the powder mixture.

(2) When the liquid-phase sintering aid present in the powder mixture is either too much or too little, a second alloy phase (R_2Co_7 or R_2Co_{17}) generally appears in the sintered core. The presence of a second alloy phase causes the magnetic properties to deteriorate. The magnetic parameters vary monotonically with the relative content of the second alloy phase in the sample.

(3) When as sintered $Sm_{0.5}Pr_{0.5}Co_5$ magnets are subjected to annealing at 900°C, appearance or increase of a second alloy phase (R_2Co_7 or R_2Co_{17}, depending

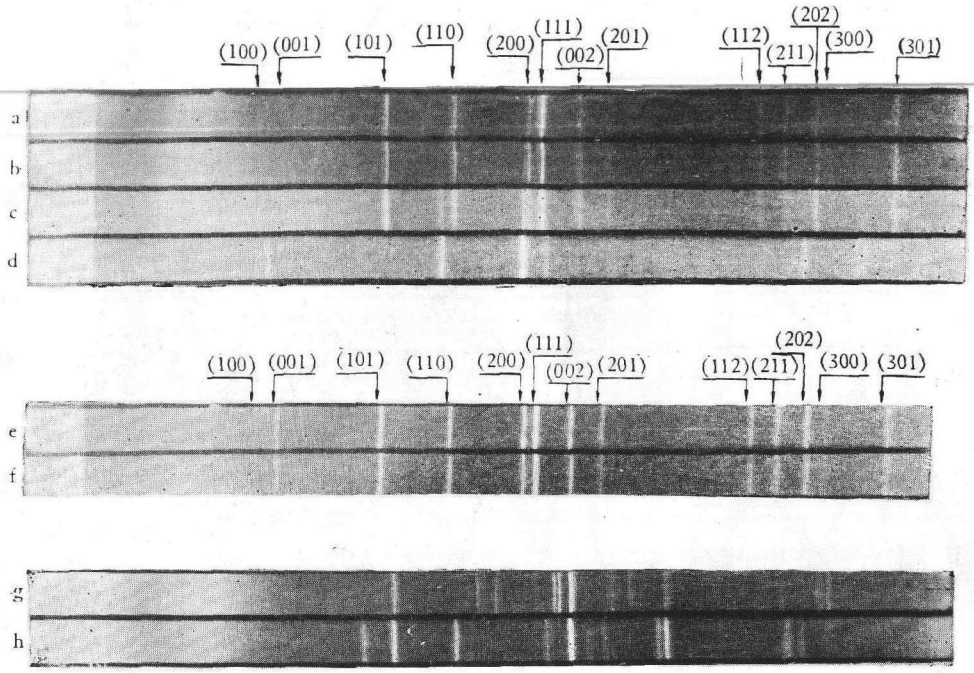

PLATE I. Guinier diffraction patterns of various samples.

a—$MM_{0.5}Sm_{0.5}Co_5$ base alloy; b—Liquid-phase sintered $MM_{0.5}Sm_{0.5}Co_5$ core from powder compact of overall Co-content of 63 % by weight; c—Mixed powder of $MM_{0.5}Sm_{0.5}Co_5$ base alloy and Sm-Co liquid-phase sintering aid, overall Co-content = 63 wt. %; d—Sm-Co liquid-phase sintering aid (60 % Sm by weight); e—Liquid-phase sintered $Sm_{0.5}Pr_{0.5}Co_5$ core from powder compact of overall Co-content of 63 % by weight; f—Liquid-phase sintered $SmCo_5$ core from powder compact of overall Co-content of 63 % by weight; g—Skin layer of the liquid-phase sintered $MM_{0.5}Sm_{0.5}Co_5$ magnet (complementary to b); h—Residue of mixed powder of $MM_{0.5}Sm_{0.5}Co_5$ base alloy and Sm-Co liquid-phase sintering aid burnt in air at 1095 °C.

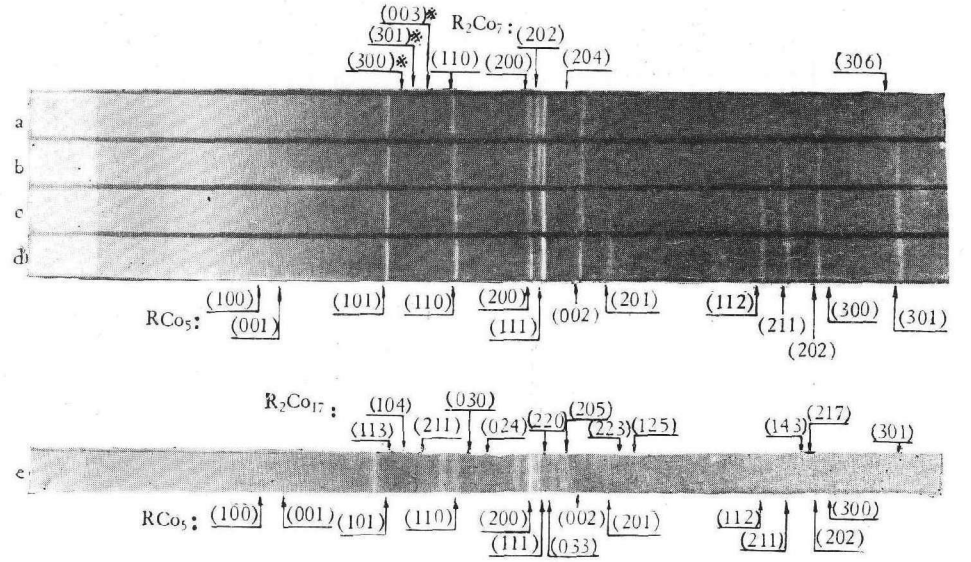

PLATE II. Guinier diffraction patterns of liquid-phase sintered $Sm_{0.5}Pr_{0.5}Co_5$ cores from powder compacts of various overall Co-contents.

a—59 % Co (by weight); b—61 % Co; c—63 % Co; d—65 % Co; e—67 % Co.

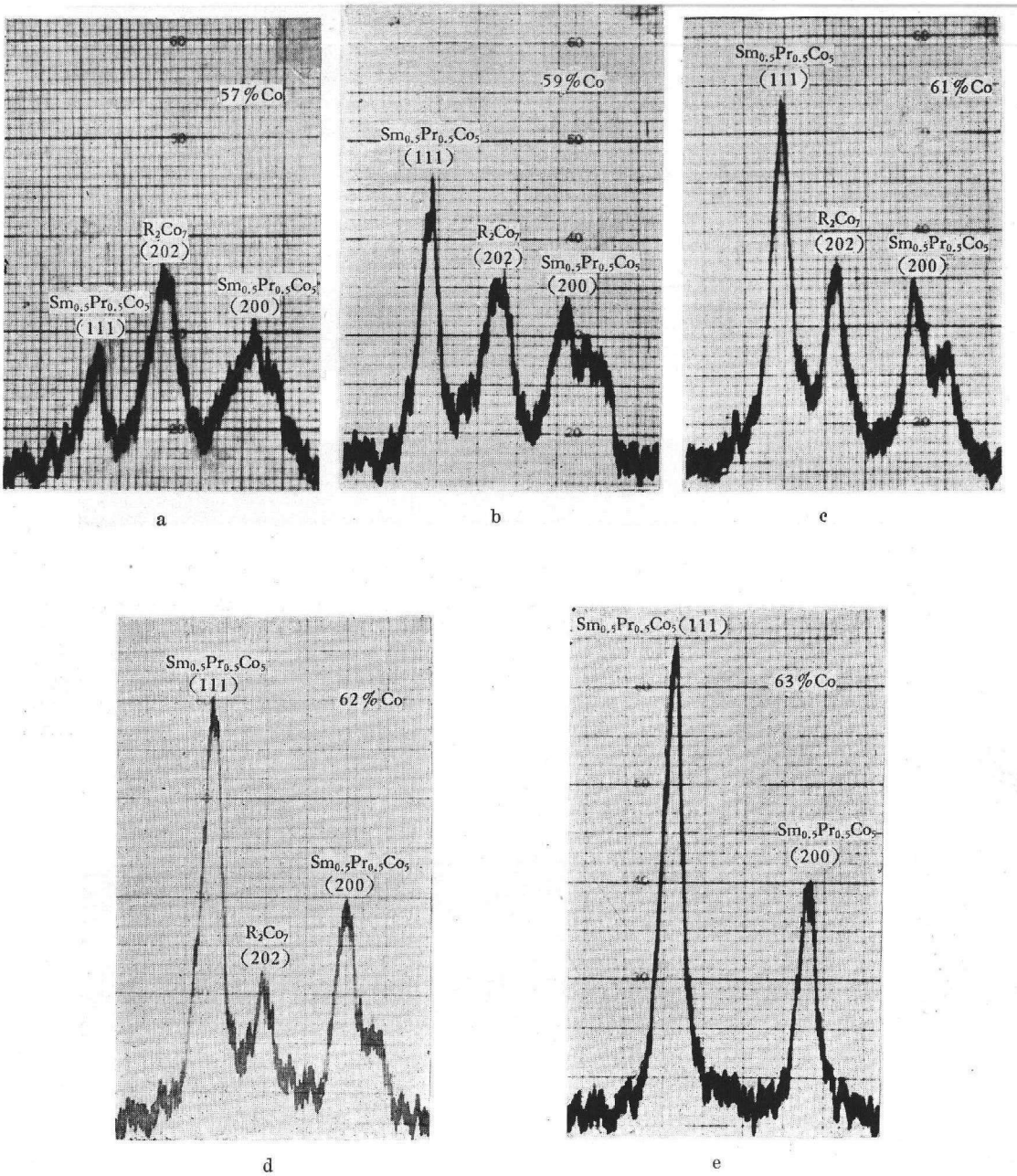

PLATE III. Recorded diffraction lines of liquid-phase sintered $Sm_{0.5}Pr_{0.5}Co_5$ cores from powder compacts of various overall Co-contents.

a—59 % Co (by weight); b—59 % Co; c—61 % Co; d—62 % Co; e—63 % Co.

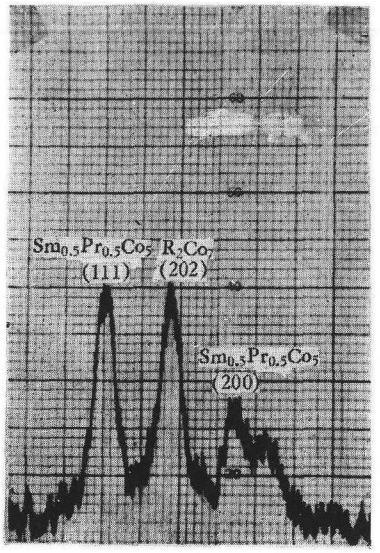

a

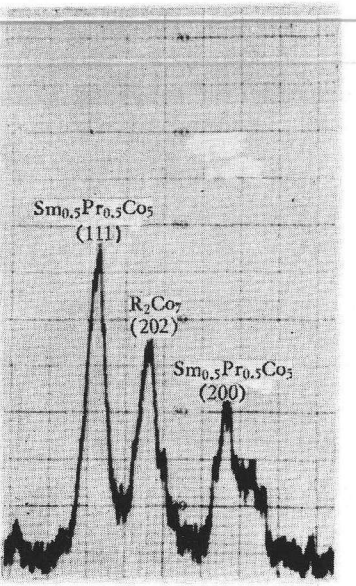

b

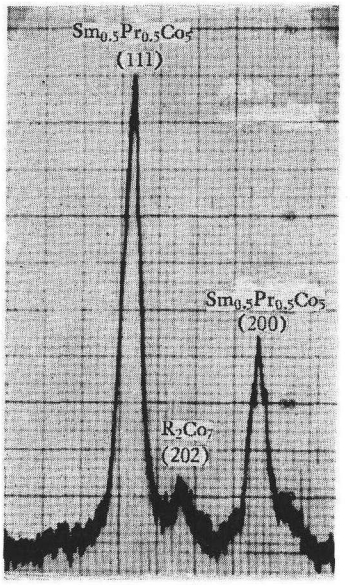

c

PLATE IV. Recorded diffraction lines of a part of the samples used to obtain Plate III after the samples are subjected to annealing at 900 °C for 8 hrs.

a—59 % Co; b—61 % Co; c—63 % Co.

on the composition of the sample) results, with an accompanied deterioration of the magnetic properties. This is probably due to the existence of a narrow homogeneity region about the stoichiometric composition RCo_5 at high temperatures. The main alloy phasee of composition RCo_{5-x} or RCo_{5+x}, which is preserved in the sintering process, breaks up on annealing to form RCo_5 and R_2Co_7 or R_2Co_{17}.

References

[1] Benz, M. G. & Martin, D. L.: *J. Appl. Phys.*, **43**(1972), 3165.
[2] Schweizer, J., Strnat, K. J. & Tsuei, J. B. Y.: *IEEE Trans. on Magnetics*, MAG-7 (1971), 429.
[3] Strnat, K. J.: *AIP Conf. Proc.*, (1972), No. 5, 1047.
[4] Khan, Y. & Feldmann, D.: *J. Less-Common Metals*, **31**(1973), 211.
[5] Khan, Y. & Mueller, B.: *Ibid.*, **32**(1973), 39.